Two-stage Stochastic Optimization for the Extended Aircraft Arrival Management Problem Under Uncertainty

Fabian Bastin, Sonia Cafieri, Ahmed Khassiba, Marcel Mongeau

Two-stage Stochastic Optimization for the Extended Aircraft Arrival Management Problem Under Uncertainty

Fabian Bastin and Sonia Cafieri and Ahmed Khassiba and Marcel Mongeau

Abstract This chapter reviews recent developments to manage aircraft arrivals in the context of extended arrival manager systems, for which uncertainty is significant when predicting expected times to start the approach phase and landing times. An original high-level multi-stage stochastic optimization formulation, considering several air network points of interest, is first introduced, taking account of practical operational constraints. The remaining of the chapter focuses on the two-stage special case, which corresponds to recent studies on the aircraft arrival management problem. A landing order is decided at a specific air network point known as the *initial approach fix*, or IAF (first stage), and a recourse cost is proposed so as to ensure that aircraft separation constraints are satisfied at the landing runway (second stage). Multiple possible IAF points are considered as well as the possibility to delay the departure of on-ground aircraft. Finally, this study proposes new analyses (validation score and impact of inclusion of chance constraints in the first stage) of numerical experiments performed on realistic instances based on Paris-Charles de Gaulle arrival data. We discuss numerical results and exhibit that the stochastic solutions are more robust than their deterministic counterparts.

Fabian Bastin
CIRRELT and DIRO, Université de Montréal,
e-mail: bastin@iro.umontreal.ca

Sonia Cafieri
ENAC, Université de Toulouse,
e-mail: sonia.cafieri@enac.fr

Ahmed Khassiba
Capgemini Engineering,
e-mail: ahmed.khassiba@capgemini.com

Marcel Mongeau
ENAC, Université de Toulouse,
e-mail: marcel.mongeau@enac.fr

1 Introduction

We address an operations research problem, the aircraft arrival scheduling problem, which is crucial in air traffic management, as one of its major bottlenecks is the airport landing runways (Kistan et al., 2017). We take account of the arriving aircraft a long time before landing, so as to have more degrees of freedom to schedule landings. However, increasing thereby the considered time horizon brings more uncertainty that needs to be handled.

The aircraft arrival scheduling problem consists in determining a sequence of a set of aircraft and their schedule on reference air-traffic route points in the *terminal maneuvering area* (air space around the destination airport), as well as a landing schedule satisfying time-window constraints and safety separation constraints for any pair of aircraft. The separation constraints are of particular importance in air traffic control. When aircraft are airborne, a fixed minimal inter-aircraft distance (typically 5 NM, where NM stands for Nautical Mile, which corresponds to approximately 1.85 km) constraint must be satisfied, whereas at the runway this safety distance depends on the types of aircraft involved, due to so-called *wake-vortex turbulence* (which affects more severely a light aircraft landing immediately after a large aircraft) (Breitsamter, 2011). Several other operational features can be taken into account, allowing thereby one to assess better the quality of the aircraft arrival schedule.

We assume that each aircraft considered in the problem comes with an initial (default) reference route from its origin airport to its destination airport. We also assume that the following information is known for each aircraft: speed, initial (planned) departure time, and wake-vortex turbulence category (light, medium, or heavy), as introduced by the International Civil Aviation Organization (ICAO) (Antolovic and Franjkovic, 2020).

The framework of the aircraft arrival scheduling problem addressed in this chapter is related to the AMAN (Arrival MANager) decision-aid tool (Hasevoets and Conroy, 2010) currently in use by air traffic controllers. Air traffic controllers can issue various possible instructions to pilots in order to impose delays (positive or negative) to flights and thereby satisfy the constraints and improve the schedule. Among these instructions used to implement the solution proposed by AMAN, let us mention aircraft speed reduction, path stretching or shortening, or *stack holding* (airborne aircraft "waiting room", as depicted in Figure 1). Typically, scheduling starts around 30 minutes before landing. The problem addressed here is in the more general *extended-AMAN* context: the scheduling horizon is extended to aircraft that are within 200–500 NM from runway threshold (Itoh et al., 2017). This corresponds to 2–3 hours before landing (Tielrooij et al., 2015), yielding more uncertainty on predicted approach and landing times.

We first consider the even more general operational setup that involves a set of aircraft flying over multiple *route points*, which are the vertices of the network of air routes. In particular, before landing, each aircraft must fly through a route point called *Initial Approach Fix* (IAF) where aircraft are sequenced by air-traffic controllers, using current decision-aid tools such as AMAN. The terminal maneuvering area of

an airport can have a single IAF, gathering all arriving aircraft prior to landing, or several IAFs. Typically, aircraft sharing neighboring routes go through a same IAF, as illustrated on Figure 1 for the case involving two IAFs. In the case involving several IAFs, aircraft are often simply assigned to the IAF closest to their arrival route. However, in practice, air traffic controllers can change an aircraft's IAF assignment to improve the arrival sequence, as explored in Khassiba et al. (2022). Additionally, the flight *status* of each considered aircraft can be taken into account, distinguishing between an aircraft that is still at its departure airport gate from one that is already airborne. More precisely, when making decisions on arrival times to IAFs, the former can be delayed on ground if needed.

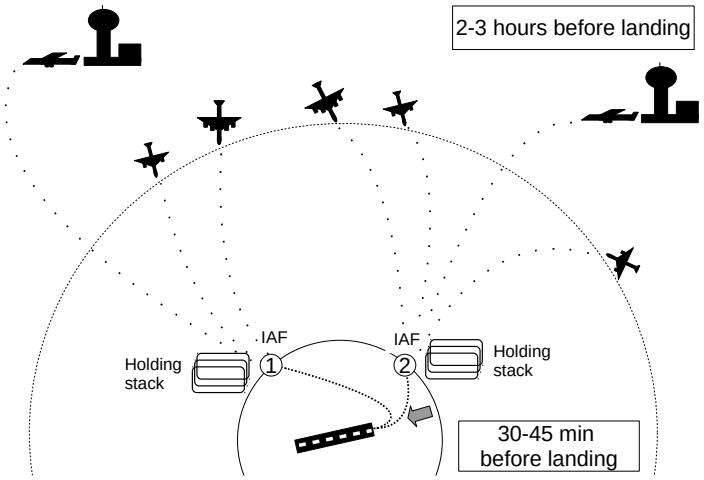

Fig. 1 Terminal maneuvering area and airport approach

The sequencing and scheduling aircraft landing problem has been studied since the 1970's (see, for instance, Dear (1976); Psaraftis (1978); Dear and Sherif (1991)). The deterministic case has received the most attention (Balakrishnan and Chandran, 2010; Beasley et al., 2000) until recently. We refer the reader to Bennell et al. (2011) and Ikli et al. (2021) for recent surveys. However, the importance of taking uncertainty into account in air traffic management is now well recognized (Shone et al., 2021).

Specific optimization paradigms such as two-stage stochastic programming (Birge and Louveaux, 2011), have been applied to the aircraft scheduling problem under uncertain arrival times with short operational horizon (Liu et al., 2018; Sölveling and Clarke, 2014; Sölveling et al., 2011). Extensions to various types of disturbances and uncertainties have also been addressed in a number of papers related to aircraft scheduling in the terminal maneuvering area (Huo et al., 2021; Samà et al., 2014; Scala et al., 2021; Vié et al., 2022). Khassiba et al. (2019, 2020, 2022) introduce two-stage stochastic mixed-integer programming models to address the problem of

arrival management under uncertainty with an extended operational time horizon. In the first-stage problem, target times of arrival of aircraft at the IAF, and a target IAF aircraft sequence are determined. Actual arrival times at the IAF are assumed to deviate randomly from these target times, following known probability distributions. They are assumed to be revealed at the second stage, so that the second-stage problem determines landing times (keeping the same IAF aircraft sequence) in view of minimizing a cost function. The numerical experiments presented in Khassiba et al. (2019, 2020) show that the obtained stochastic solutions are more robust to the uncertainty occurring within the 2–3 hours before landing than their deterministic counterparts.

In Khassiba et al. (2019, 2020), one single IAF is considered. In Khassiba et al. (2019, 2020), all aircraft are considered airborne, while on-ground vs. airborne flight status are taken into account in Khassiba et al. (2022).

The present chapter first introduces, in Section 2, our main contribution: a detailed high-level multi-stage stochastic optimization formulation of the extended aircraft arrival management problem under uncertainty that can consider *several* air network points of interest (previous literature commonly considers at most two such points: the IAF and the landing runway). It takes into account other practical operational features such as the airborne/on-ground status of aircraft, and the possibility to delay the departure of on-ground aircraft, as this was also the case for the two-stage study of Khassiba et al. (2022). The focus of this chapter is then made on the two-stage special case which corresponds to recent studies on the aircraft arrival management problem (Khassiba et al., 2019, 2020, 2022): a landing order is decided at one particular air network point, the IAF (first stage), and a recourse cost is proposed so as to ensure that aircraft separation constraints are satisfied at the landing runway (second stage). Section 3 presents the sample average approximation (SAA) method (Shapiro, 2021) that is applied to perform numerical tests. Section 4 reports new numerical experiments on realistic instances based on Paris-Charles de Gaulle arrival data, with discussions on the appropriate number of scenarios, the value of the stochastic solutions, and the effect of using chance constraints. Section 5 presents conclusions and propositions of avenues for future research.

2 Optimization Models

This section first introduces the high-level multi-stage stochastic optimization model we are proposing for the extended aircraft arrival management problem under uncertainty. Details on the two-stage special case are then presented, along with the full two-stage stochastic optimization model on which we shall rely for our numerical experiments. It is a concise form (without the detailed description of all the operational constraints, and keeping the most generic setting) of the two-stage model presented in Khassiba et al. (2022). A summary of the notations used is provided in Appendix.

2.1 High-level Multi-stage Stochastic Optimization Model

The last decades have experienced a fast increase of air traffic, and while the aviation industry had to reduce significantly its activities during the Covid-19 pandemic, the demand has returned to high levels, raising various challenges in air traffic management (Kistan et al., 2017; Bolić and Ravenhill, 2021). As underlined by Itoh et al. (2021), a current research avenue to improve aircraft arrival scheduling is the use of a multi-stage decision sequence model, while accounting for uncertainty. They also suggest to consider time management rather than flow management.

In line with these considerations, we introduce a new model, as general as possible, using a stochastic dynamic programming formulation over $K(\geq 2)$ stages. Each stage is indexed by $k = 1, 2, \ldots, K$. We assume that for each stage $k = 1, 2, \ldots, K-1$, we are given the number, $n^{(k)}$, of considered aircraft, and $\mathcal{A}^{(k)}$, the associated index set of aircraft. The latter is partitioned further into two subsets: $\mathcal{A}_G^{(k)}$ and $\mathcal{A}_A^{(k)}$, the index set corresponding to the aircraft that are still on the ground at stage k, and the index set related to the aircraft that are airborne at stage k, respectively. We also assume that we are given an index set, $\mathcal{I}^{(k)}$, of possible routes for the aircraft in $\mathcal{A}^{(k)}$. We suppose here that $n^{(k)}$ can change over time as with extended aircraft arrival management systems, airborne aircraft can appear on the radar at a stage $k > 1$. Similarly, additional on-ground aircraft may have to be considered from a stage $k > 1$, for instance if their planned departure time have been delayed.

At each stage k, the following decisions must be made. First, one decides for each aircraft $a \in \mathcal{A}^{(k)}$, whether its *route* should be modified (the route is represented by a sequence of *waypoints*, which are air network vertices) chosen within $\mathcal{I}^{(k)}$. Second, one decides an aircraft sequence at a particular future air route point of interest (that we shall call *target point*) associated to stage k. Third, one decides a target time, within a given time window, for each aircraft, $a \in \mathcal{A}^{(k)}$, to reach this (next-stage) target point. Finally, one decides a target take-off time for each on-ground aircraft $a \in \mathcal{A}_G^{(k)}$.

More precisely, for $k = 1, 2, \ldots K-1$, the kth-stage problem **decision vector**, noted $x^{(k)}$, reads:

$$x^{(k)} = (z^{(k)}, t^{(k)}, \delta^{(k)}, \zeta^{(k)}),$$

where $z^{(k)} \in \mathbb{R}^{n^{(k)}}$ is the vector of target-time variables (associated to the next-stage target point); $t^{(k)} \in \mathbb{R}^{|\mathcal{A}_G^{(k)}|}$is the vector of target take-off time variables for on-ground aircraft; $\delta^{(k)}$ is a vector of discrete variables (*sequencing variables*: one binary variable for each possible pair of aircraft) used to decide a sequence of aircraft at the next-stage target point, and $\zeta^{(k)}$ is the vector of the aircraft route assignment variables (each of its $n^{(k)}$ components is a route index from $\mathcal{I}^{(k)}$). The last-stage decision vector, $x^{(K)}$, is particular: it is simply the vector of target landing time variables, $z^{(K)} \in \mathbb{R}^{n^{(K-1)}}$.

In this general multi-stage context, the last stage, K, is indeed particular: it focuses on the decision related to a special target point: the (landing) runway threshold. The penultimate stage, $K-1$, is concerned with another special target point: the IAF.

Stage $K-1$ thereby concentrates on the decisions related to the aircraft passing through their assigned IAF. For example, deciding a route assignment $\zeta_a^{(K-1)}$ for aircraft $a \in \mathcal{A}^{(K-1)}$, boils down to deciding whether the initial IAF assignment for aircraft a should be modified. In a context involving more than two stages, the previous stage, $K-2$, could involve deciding whether yet another specialized air-traffic-control waypoint, the merge point, planned on the initial route of a, should be modified or not.

At each stage $k = 1, 2, \ldots, K$, we define a state vector, $s^{(k)}$, whose ath component,

$$s_a^{(k)} = (p_a^{(k)}, r_a^{(k)}, v_a^{(k)}, \kappa_a^{(k)}, \chi_a^{(k)}),$$

gives the following five features related to aircraft $a \in \mathcal{A}^{(k)}$: $p_a^{(k)}$ is the position of aircraft a at stage k, $r_a^{(k)}$ is the *current* (at stage k) reference route of aircraft a, $v_a^{(k)}$ is its speed at stage k, $\kappa_a^{(k)}$ gives the status (on-ground or airborne) of a at stage k, and $\chi_a^{(k)}$ stores other useful characteristics of aircraft a (that does not change through the stages in the current study) such as its wake-vortex turbulence category (light, medium, or heavy). Remark that at stage $k = 1$ the state vector, $s_a^{(1)}$, is known for every aircraft $a \in \mathcal{A}^{(1)}$, and similarly for any new aircraft appearing at some subsequent stage (*pop-up flight*).

Let us introduce, for each stage $k = 1, 2, \ldots, K$, the following notation: the objective function $f^{(k)}$, capturing the operating costs at stage k (for instance, penalties on the deviations from the target times), the separation-constraint mapping $S^{(k)}$ to be satisfied by the aircraft pairs at the next-stage target points, the time-window constraint mapping $T^{(k)}$ representing the feasible passing times at next-stage target points, and a feasible set $\mathcal{X}^{(k)}$ to account for the domain definition of the vector of decision variables, $x^{(k)}$.

The stochastic dynamic optimization model therefore reads as follows, for $k = 1, 2, \ldots, K$:

$$V^{(k)}(s^{(k)}) = \min_{x^{(k)}} f^{(k)}(x^{(k)}, s^{(k)}) + \mathbb{E}_{\boldsymbol{\xi}^{(k+1)}}[V^{(k+1)}(\boldsymbol{s}^{(k+1)}) \mid s^{(k)}] \tag{1}$$

$$\text{s.t.} \quad T^{(k)}(x^{(k)}, s^{(k)}) \leq 0 \quad \text{time windows at next-stage target points} \tag{2}$$

$$S^{(k)}(x^{(k)}, s^{(k)}) \leq 0 \quad \text{separation at next-stage target points} \tag{3}$$

$$x^{(k)} \in \mathcal{X}^{(k)}, \tag{4}$$

and $V^{(K+1)}(\cdot) = 0$. For $k = 1, \ldots, K-1$, the state transition function is

$$s^{(k+1)} = g^{(k)}(x^{(k)}, s^{(k)}, \boldsymbol{\xi}^{(k+1)}),$$

where $\boldsymbol{\xi}^{(k+1)}$ is some random vector capturing the uncertainty affecting the problem at the next stage (stage $k+1$). In line with other studies (see for instance Itoh et al. (2021)), in our context, $\boldsymbol{\xi}^{(k+1)}$ captures the random time deviations (advances or delays) affecting the aircraft with respect to their target times at their next target points, due to various operational and environmental factors, such as the wind, and

limited operational adjustments in order to extend engine lifetime. Other sources of uncertainty could also be taken into account, at the price of additional modeling and computational complexity.

2.2 Two-stage Special Case

Practitioners commonly concentrate on decisions related to the last two target points: the IAF and the runway threshold. Two-stage stochastic optimization is suitable for this operational context. The exposition can be generalized to more than two stages as introduced above but specific operational constraints (including the smooth management of aircraft engine to optimize its lifetime) renders the two-stage framework best fit to this application. For this reason, and in order to simplify the presentation, in the sequel, we set $K = 2$ (two-stage optimization): the first target point ($k = 1$) is the IAF, and the second ($k = 2$) is the runway threshold. Also, for notational simplicity, we shall use $x \in \mathcal{X}$ instead of our general multi-stage notation $x^{(1)} \in \mathcal{X}^{(1)}$, and $y \in \mathcal{Y}$ instead of $x^{(2)} \in \mathcal{X}^{(2)}$. Regarding uncertainty, we shall simply use $\boldsymbol{\xi}$ instead of $\boldsymbol{\xi}^{(2)}$ (and there is no random variable $\boldsymbol{\xi}^{(1)}$ in the special case we are considering here).

The **first-stage** problem considers aircraft that are 2–3 hours away from the IAFs (see Figure 1), when each aircraft time to cross the IAF is still uncertain. The first-stage problem aims thereby at deciding a target aircraft sequence, together with an IAF affectation and an IAF target time for each aircraft, under the constraints of IAF time windows and safe separation of aircraft at IAF. Depending on the modeling assumptions, for each aircraft the IAF may be selected before solving the optimization model (typically, the closest IAF), or explicitly be a first-stage decision variable. The **second-stage** problem deals with the same set of aircraft, now close to the IAF, when the actual time to cross the IAF is known for each aircraft. The second-stage problem aims at deciding a target landing time for each aircraft, under the constraints of landing time windows and safe aircraft separations at the runway.

This leads to the following two-stage stochastic optimization model:

$$\min_{x=(z,t,\delta,\zeta)} f^{(1)}(x) + \mathbb{E}_{\boldsymbol{\xi}}\left[Q(x,\boldsymbol{\xi})\right] \tag{5}$$

$$\text{s.t.} \quad T^{(1)}(z,t,s^{(1)}) \leq 0 \qquad \text{time windows at IAF} \tag{6}$$

$$S^{(1)}(x,s^{(1)}) \leq 0 \qquad \text{separation at IAF} \tag{7}$$

$$x \in \mathcal{X}, \tag{8}$$

$$\text{with} \quad Q(x,\xi) = \min_{y} f^{(2)}(y,\xi) \tag{9}$$

$$\text{s.t.} \quad T^{(2)}(y,s^{(2)}) \leq 0 \qquad \text{time windows at runway} \tag{10}$$

$$S^{(2)}(y,s^{(2)}) \leq 0 \qquad \text{separation at runway} \tag{11}$$

$$y \in \mathcal{Y}, \tag{12}$$

where

$$s^{(2)} = g(x, s^{(1)}, \xi),$$

g is the transition function that updates the state vector from stage 1 to stage 2, and where the first-stage vector of decision variables, $x = (z, t, \delta, \zeta)$ and the second-stage vector of decision variables, y, are defined as follows.

Let $\mathcal{A}$ be the index set of all aircraft, which is partitioned into the index sets $\mathcal{A}_A$ and $\mathcal{A}_G$, respectively the subset of airborne and the subset of on-ground aircraft, and let $\mathcal{I}$ be the index set of IAFs. At the first stage, one decides:

- a target arrival time for each aircraft $a \in \mathcal{A}$ at its assigned IAF, which is denoted by $z \in \mathbb{R}^{|\mathcal{A}|}$;
- a target take-off time for each on-ground aircraft, $a \in \mathcal{A}_G$, represented by the optimization variable $t \in \mathbb{R}^{|\mathcal{A}_G|}$;
- a target sequence of all aircraft $a \in \mathcal{A}$ which is coded in the binary optimization variable $\delta \in \{0,1\}^{|\mathcal{A}|\times|\mathcal{A}|}$;
- the assignment of an IAF $i \in \mathcal{I}$ for each aircraft $a \in \mathcal{A}$, encoded via the binary optimization variables $\zeta \in \{0,1\}^{|\mathcal{A}|\times|\mathcal{I}|}$.

At the second stage, one decides:

- a target landing time for each aircraft $a \in \mathcal{A}$ which is denoted by $y \in \mathbb{R}^{|\mathcal{A}|}$.

Remark that for each IAF, δ specifies the sequence order, and z specifies each aircraft time at its IAF, while y encodes each aircraft landing time. The landing sequence must be *coherent* with the IAF sequences, since aircraft coming from a same IAF cannot overtake each other.

The objective and constraint functions of the general formulation (5)–(12) are made explicit in the next subsections, following the model introduced in Khassiba et al. (2022). Note that in Khassiba et al. (2022) some variants of the problem (depending on the considered operational setup) are considered and associated models are proposed. Here we focus only on the two-stage model that was identified as the closest to the air traffic operating environment, i.e., the one incorporating decisions on multiple IAF points and taking into account multiple aircraft flight status, and we present it in a concise way which is moreover easier to generalize.

2.2.1 Objective Functions

The objective function in (5) is the sum of the first-stage function that captures the time-deviation costs at take-off for the on-ground aircraft, and the recourse cost, expressed as the the expectation of the optimal value, $Q(x, \boldsymbol{\xi})$, of the second-stage objective function. Note that we could weigh the recourse cost by multiplying it by a parameter $\lambda \in \mathbb{R}^+$, as done in Khassiba et al. (2020), but for simplicity, we keep λ equal to one in the following.

Given a scenario ξ (a realization of the random vector $\boldsymbol{\xi}$), actual times of arrival at the IAFs are assumed to be known, and for each IAF, the corresponding aircraft sequence computed at the first stage is enforced and only the target landing time, y_a, is to be decided for each aircraft $a \in \mathcal{A}$. The complete landing sequence, gathering the aircraft coming from any IAF, is thus implicitly determined by the landing times. The second-stage objective function corresponds to the total time-deviation (delay and advance) cost incurred during the *en-route* (relative here to the part of the flight that takes place before the IAF) and the *approach* (after the IAF) phases. As in Khassiba et al. (2022), the time-deviation cost depends on the deviation duration, and the delay cost is determined according to the reference values proposed in the report authored by Cook and Tanner (2015), while the approach cost is minimized with respect to the landing times y_a for each $a \in \mathcal{A}$. The second-stage objective function is typically a sum of convex piecewise linear functions, and can be easily replaced by an equivalent linear objective function (Bradley et al., 1977, Section 9.2).

Alternative formulations, and related interpretations are possible (see for instance Khassiba et al. (2019, 2020)), but are not considered here.

2.2.2 Time-window Constraints at IAF

Let us consider an aircraft $a \in \mathcal{A}$. The time-window constraint (6) expresses that its *target IAF time*, z_a, must lie within a time window $\left[E_a^i,\ L_a^i\right]$, where E_a^i and L_a^i denote respectively the *earliest time* and the *latest time* of a at its assigned IAF $i \in \mathcal{I}$:

$$z_a \in \left[E_a^i,\ L_a^i\right].$$

Recall that during the en-route flight phase, with 2–3 hour look-ahead time, it is possible to expedite or delay aircraft a by a given amount of time through its speed change. These earliest and latest times can be computed by taking into account the *maximal possible time saving*, and the *maximal possible delay* for aircraft a during its en-route phase, denoted as $\underline{d}_a^R$ and $\overline{d}_a^R$ respectively, as follows:

$$E_a^i = P_a^i - \underline{d}_a^R$$
$$L_a^i = P_a^i + \overline{d}_a^R,$$

where P_a^i is the *planned IAF time* of aircraft a at IAF i.

Remark that P_a^i can be determined, and hence E_a^i and L_a^i can be further made explicit, according to the flight status (airborne ou on-ground) of aircraft a. Let us first observe that the initially-assigned IAF of aircraft a is assumed to be the IAF $i^* \in \mathcal{I}$ that is closest to the reference (initially-planned) route of a. As a consequence, deciding to assign aircraft a to an IAF j that is different from i^* ($j \in \mathcal{I} \setminus \{i^*\}$) incurs a positive rerouting delay, noted $r^{i^*j} > 0$ (with $r^{i^*i^*} = 0$). Recalling that variables ζ are used to decide the assignment of each aircraft a to an IAF i, $\sum_{j \in \mathcal{I}} r^{i^*j} \zeta_a^j$ denotes the actual rerouting delay for aircraft a.

For an airborne aircraft, $a \in \mathcal{A}_A$, and an IAF $i \in \mathcal{I}$, the planned IAF time is then straightforwardly computed from input data (the planned time to the initial IAF, denoted $P_a^{i^*}$), adding r^{i^*j} in the case where the aircraft is rerouted to an IAF different from its initial one. The time-window constraint (6) at the IAF for an airborne aircraft then reads as

$$-\underline{d}_a^R \leq z_a - P_a^{i^*} - \sum_{j \in \mathcal{I}} r^{i^*j} \zeta_a^j \leq \overline{d}_a^R.$$

For an on-ground aircraft, $a \in \mathcal{A}_G$ (still at its departure gate), the planned IAF time depends on further input data (the flight time from the origin airport of a to its initial IAF $i^* \in \mathcal{I}$, denoted $\hat{V}_a^O$) as well as on the decision variable t_a representing the target take-off time. This variable t_a is in turn bounded by taking into account the planned take-off time, P_a^{TOT}, and the maximal possible delay $\overline{d}^G > 0$ to take off: $0 \leq t_a \leq P_a^{\text{TOT}} + \overline{d}^G$. The time-window constraint at the IAF for an on-ground aircraft then reads:

$$-\underline{d}_a^R \leq z_a - t_a - \hat{V}_a^O - \sum_{j \in \mathcal{I}} r^{i^*j} \zeta_a^j \leq \overline{d}_a^R.$$

The way E_a^i and L_a^i are computed for aircraft with different flight status is detailed in Khassiba et al. (2022).

2.2.3 Separation Constraints at IAF

In the first-stage problem, a target sequence of aircraft at each IAF and target IAF times of each aircraft are determined in such a way that, for safety reasons, successive aircraft crossing the same IAF are pairwise separated by a minimal time separation, $\underline{S}$. The assignment of each aircraft $a \in \mathcal{A}$ to an IAF $i \in \mathcal{I}$ is decided through the binary decision variable ζ_a^i (whose value is equal to 1 if aircraft a is assigned to IAF i, 0 otherwise), while binary variables δ decide the landing sequence of all aircraft during the second stage. This in turn determines the sequence of arrivals at each IAF since the corresponding relative order is kept unchanged for landing at the runway. More precisely, a binary decision variable δ_{ab} for each ordered pair of aircraft $(a, b) \in \mathcal{A} \times \mathcal{A}$, $a \neq b$ is defined as follows:

$$\delta_{ab} = \begin{cases} 1 & \text{if aircraft } a \textbf{ lands before} \text{ aircraft } b, \\ 0 & \text{otherwise.} \end{cases}$$

Remark that these variables are defined, like in Khassiba et al. (2022), as in scheduling theory, where *direct* precedence is *not* required, as opposed to what is done in Khassiba et al. (2020), where the sequencing variables are defined so as to indicate *direct precedence* between a pair of aircraft (like in the classical model for the traveling salesman problem).

In order to formulate the separation constraints at each IAF, we further introduce the following auxiliary binary decision variables for each pair of aircraft $(a, b) \in \mathcal{A} \times \mathcal{A}$, $a \neq b$:

$$\phi_{ab} = \begin{cases} 1 & \text{if aircraft } a \text{ and } b \text{ are assigned to a same IAF,} \\ 0 & \text{otherwise,} \end{cases}$$

together with defining constraints:

$$\begin{aligned} \sum_{i \in \mathcal{I}} \zeta_a^i = 1 \qquad & a \in \mathcal{A} \\ \phi_{ab} = \phi_{ba} \quad (a,b) \in \mathcal{A} \times \mathcal{A}, \qquad & a < b \\ \phi_{ab} \geq \zeta_a^i + \zeta_b^i - 1 \qquad & i \in \mathcal{I}\,, \quad (a,b) \in \mathcal{A} \times \mathcal{A}, \quad a < b \\ \delta_{ab} + \delta_{ba} = 1 \qquad & (a,b) \in \mathcal{A} \times \mathcal{A}, \quad a < b. \end{aligned}$$

Finally, the first-stage constraints expressing pairwise aircraft separation at each IAF takes the form:

$$z_b \geq z_a + \underline{S} - M_{ab}(2 - \phi_{ab} - \delta_{ab}) \qquad (a,b) \in \mathcal{A} \times \mathcal{A}, \quad a \neq b,$$

where M_{ab} is a sufficiently large constant defined for each pair $(a,b) \in \mathcal{A} \times \mathcal{A}$ such that $a \neq b$.

2.2.4 Time-window Constraints at Runway

Let us consider an aircraft $a \in \mathcal{A}$. The target landing time, y_a, must lie within a time window:

$$y_a \in [E_a,\, L_a]\,,$$

where E_a and L_a are its earliest and latest landing times, computed as the actual time of a at its assigned IAF i when uncertainty is revealed: $z_a + \xi$, to which we add the minimal and maximal flight times from the IAF i to the runway threshold. These minimal and maximal flight times are respectively defined as

$$\underline{V_a}^{\,i} = \hat{V_a}^{\,i} + \underline{d}_a^T, \qquad \overline{V_a}^{\,i} = \hat{V_a}^{\,i} + \overline{d}_a^T,$$

where, $\hat{V_a}^{\,i}$ is the unconstrained flight time of the aircraft a from i to the runway threshold, $\overline{d}_a^T$ is the maximal possible delay during the approach phase, and $\underline{d}_a^T$ is the maximal possible time saving during the approach phase. Recall that the assigned IAF i of each aircraft a is decided through binary variables ζ_a^i, for all i. Hence, minimal and maximal flight times from the IAF to the runway threshold are to be selected according to the value of such variables ζ. Finally, time windows constraints at runway read:

$$\sum_{i \in \mathcal{I}} \underline{V_a}^{\,i} \zeta_a^i \leq y_a - (z_a + \xi_a) \leq \sum_{i \in \mathcal{I}} \overline{V_a}^{\,i} \zeta_a^i.$$

2.2.5 Separation Constraints at Runway

In the second-stage problem, when uncertainty on target times at the IAFs is revealed, for each aircraft, we decide on a target time, y_a, at the runway threshold. A minimal time separation, S_{ab}, must then be satisfied for each pair of aircraft landing successively:

$$y_b \geq y_a + S_{ab} - M^L_{ab}(1 - \delta_{ab}) \quad (a, b) \in \mathcal{A} \times \mathcal{A}, \quad a \neq b,$$

where M^L_{ab} is a sufficiently large constant defined for each $(a, b) \in \mathcal{A} \times \mathcal{A}$ $(a \neq b)$, and where S_{ab} is determined from minimal separation distances (Gerz et al., 2002; Breitsamter, 2011). These separation distances are defined according to the wake-vortex turbulence category of aircraft a and that of aircraft b as introduced by the International Civil Aviation Organization: heavy (H), medium (M), and light (L) (Antolovic and Franjkovic, 2020). They are converted into minimal *time* separations, and reported in Table 1.

Table 1 Final-approach separations (in seconds) at runway according to wake-vortex turbulence categories of the leader aircraft, l, and the follower aircraft, f

	H_f	M_f	L_f
H_l	96	157	207
M_l	60	69	123
L_l	60	69	82

2.3 The Two-stage Stochastic Optimization Model

The two-stage stochastic optimization model of the extended aircraft arrival management under uncertainty presented above (and introduced in Khassiba et al. (2022)) can be summarized as follows:

$$\min_{\substack{z,t,\delta,\\ \zeta,\phi}} \sum_{a \in \mathcal{A}_G} f^{\mathrm{G}}_a \left(t_a - P^{\mathrm{TOT}}_a\right) + \mathbb{E}_{\xi}[Q(z, t, \zeta, \delta, \boldsymbol{\xi})] \tag{13}$$

$$\text{s.t.} \sum_{i \in \mathcal{I}} \zeta^i_a = 1 a \in \mathcal{A} \tag{14}$$

$$\phi_{ab} = \phi_{ba}(a, b) \in \mathcal{A} \times \mathcal{A}, a < b \tag{15}$$

$$\phi_{ab} \geq \zeta^i_a + \zeta^i_b - 1 i \in \mathcal{I}, (a, b) \in \mathcal{A} \times \mathcal{A}, a < b \tag{16}$$

$$\delta_{ab} + \delta_{ba} = 1 (a, b) \in \mathcal{A} \times \mathcal{A}, a < b \tag{17}$$

$$z_b \geq z_a + \underline{S} - M_{ab}(2 - \phi_{ab} - \delta_{ab})(a, b) \in \mathcal{A} \times \mathcal{A}, a \neq b \tag{18}$$

$$-\underline{d}_a^R \le z_a - t_a - \hat{V}_a^O - \sum_{j\in\mathcal{I}} r^{i^*j}\zeta_a^j \le \overline{d}_a^R \; i^* \in \mathcal{I}, a \in \mathcal{A}_G^{i^*} \tag{19}$$

$$-\underline{d}_a^R \le z_a - P_a^{i^*} - \sum_{j\in\mathcal{I}} r^{i^*j}\zeta_a^j \le \overline{d}_a^R \qquad i^* \in \mathcal{I}, a \in \mathcal{A}_A^{i^*} \tag{20}$$

$$0 \le t_a - P_a^{\text{TOT}} \le \overline{d}_a^G \qquad a \in \mathcal{A}_G \tag{21}$$

$$\zeta_a^i \in \{0,1\} \qquad i \in \mathcal{I}, a \in \mathcal{A} \tag{22}$$

$$\phi_{ab} \in \{0,1\} \qquad (a,b) \in \mathcal{A}\times\mathcal{A}, a \ne b \tag{23}$$

$$\delta_{ab} \in \{0,1\} \qquad (a,b) \in \mathcal{A}\times\mathcal{A}, a \ne b, \tag{24}$$

where

$$\begin{aligned} Q(z,t,\zeta,\delta,\xi) = \\ \min_y \sum_{a\in\mathcal{A}_G} f_a^{\text{R}}\left(z_a+\xi_a-\left(t_a+\hat{V}_a^O\right)\right) + \\ \sum_{a\in\mathcal{A}_A} f_a^{\text{R}}\left(z_a+\xi_a-P_a^{i^*}\right) + \\ \sum_{a\in\mathcal{A}} f_a^{\text{T}}\left(y_a-\left(z_a+\xi_a+\sum_{i\in\mathcal{I}}\hat{V}_a^i\zeta_a^i\right)\right) \end{aligned} \tag{25}$$

$$\text{s.t. } y_b \ge y_a + S_{ab} - M_{ab}^L(1-\delta_{ab}) \qquad (a,b)\in\mathcal{A}\times\mathcal{A}, a\ne b \tag{26}$$

$$\sum_{i\in\mathcal{I}} \underline{V_a}^i\zeta_a^i \le y_a - (z_a+\xi_a) \le \sum_{i\in\mathcal{I}} \overline{V_a}^i\zeta_a^i \qquad a\in\mathcal{A}, \tag{27}$$

and where M_{ab} and M_{ab}^L are sufficiently large (*big-M*) constants, defined for each $(a,b) \in \mathcal{A}\times\mathcal{A}$, $a \ne b$, and whose value can be estimated from input data (see Khassiba et al. (2022)).

The first-stage objective function (13), to be minimized, is the sum of the total at-gate time deviation and the expectation of the second-stage objective function (see Subsection 2.2.1). Constraints (14)–(17) are defining constraints on variables ζ, ϕ and δ (see Subsection 2.2.3). Constraints (18) ensure separation (in terms of target IAF times) for any pair of successive aircraft assigned to a same IAF (Subsection 2.2.3). Constraints (19) and (20) are time-window constraints for on-ground and airborne aircraft, respectively (see Subsection 2.2.2). Constraints (21) ensure that the take-off time of an on-ground aircraft is chosen in the appropriate time window. Constraints (22), (23), and (24) simply stipulate that the decision variables ζ_a^i, ϕ_{ab} and δ_{ab} are binary.

The second-stage objective function (25), to be minimized, is the total time-deviation (delay and advance) cost during the en-route and the landing phases. Constraints (26) are separation constraints at runway between any pair of landing aircraft (see Subsection 2.2.5). Constraints (27) ensure, for a given aircraft, that its landing time between its assigned IAF and the runway, lies within an appropriate time window (see Subsection 2.2.4).

Remark.

The first-stage problem can be enriched by chance constraints expressing a protection level against any separation loss over each IAF.

Letting $0 \leq \alpha \leq 1$ be a given confidence-level parameter, and incorporating the random time deviations at the IAFs into (18), we can introduce the chance constraints

$$\mathcal{P}_{\boldsymbol{\xi}}\left(z_b + \xi_b \geq z_a + \xi_a + \underline{S} - M_{ab}(2 - \phi_{ab} - \delta_{ab})\right) \geq \alpha \quad (a,b) \in \mathcal{A} \times \mathcal{A}, a \neq b. \tag{28}$$

Chance constraints guarantee that any pair of aircraft are separated at the IAF after uncertainty is revealed (actual IAF time deviations with respect to target IAF times) with a probability α, at least. Thus, $1-\alpha$ represents the risk level at which a separation constraint is violated. Equivalently, we can rewrite (28) as the linear constraints

$$z_b \geq z_a + \underline{S} + F^{-1}_{\boldsymbol{\psi}_{ab}}(\alpha) - M_{ab}(2 - \phi_{ab} - \delta_{ab}) \quad (a,b) \in \mathcal{A} \times \mathcal{A}, a \neq b. \tag{29}$$

where $F_{\boldsymbol{\psi}_{ab}}(\alpha)$ is the distribution function of $\boldsymbol{\psi}_{ab} = \boldsymbol{\xi}_a - \boldsymbol{\xi}_b$. It is noteworthy that given an aircraft pair (a,b), $a \neq b$, (29) dominates the original non-buffered IAF separation constraint (18) when $F^{-1}_{\boldsymbol{\psi}_{ab}}(\alpha) > 0$.

We numerically explore the effect of such chance constraints in Section 4.4. In our setting, similar to Khassiba et al. (2020), we assume that the random deviations $\boldsymbol{\xi}_a$'s, affecting the aircraft during the en-route phase, are independent and identically distributed, whatever the aircraft status in the first phase (airborne or on-ground). Quantifying the precise distribution of uncertainty is a tricky task, especially since the random noise is not directly observable (Tielrooij et al., 2015). For the sake of simplicity, we assume that for any a in $\mathcal{A}$, $\boldsymbol{\xi}_a$ is normally distributed with variance σ^2, $\boldsymbol{\psi}_{ab}$ is normally distributed with zero mean and variance $2\sigma^2$. In this case, $F^{(-1)}_{\boldsymbol{\psi}_{ab}}(\alpha)$ is positive if and only if $\alpha > 0.5$. In a more realistic setting, that we leave as a future avenue of investigation, it is possible to consider that an on-ground aircraft, $a \in \mathcal{A}_G$, is affected by two time deviations: its actual take-off time deviates randomly from its target take-off time, t_a, and its actual IAF time deviates as well from its target IAF time, z_a.

3 Solution Method

Objective function (5) typically has no closed-form expression due to the expectation operator, hence the problem (5)–(12), referred to as the *true problem*, cannot be solved directly. A classical remedy is to sample a finite set, $\mathcal{S}$, of scenarios over the random vector $\boldsymbol{\xi}$ to produce the *sample average approximation (SAA)* problem (Shapiro, 2021). One practical difficulty of the SAA method is the determination of an appropriate size of the scenario set. Indeed, large scenario sets capture better uncertainty. However, computing times increase exponentially with the number of scenarios. An appropriate number of scenarios can be defined as the smallest

scenario-set size that ensures an acceptable representation level of the uncertainty. After solving a two-stage stochastic problem, it is key to validate the benefit from taking into account uncertainty, against the situation where the decision-maker computes his decision assuming mean values of the uncertain parameters. One classical metric to measure the benefit from two-stage stochastic programming over a deterministic approach is the *value of the stochastic solution*. The SAA method applied to a two-stage stochastic optimization problem is presented in Subsection 3.1. In Subsection 3.2, we develop on the metrics used in our study to quantify the appropriateness of a given scenario-set size. Subsection 3.3 presents a formal definition of the value of the stochastic solution adapted to our problem, where SAA is applied as a solution method.

3.1 Sample Average Approximation

The SAA problem can be formulated as follows:

$$\begin{aligned} \min_{x} \quad & \hat{f}(x, \mathcal{S}) = f^{(1)}(x) + \frac{1}{n_{\mathcal{S}}} \sum_{\xi \in \mathcal{S}} Q(x, \xi), \\ \text{s.t.} \quad & (6)\text{–}(8), \\ \text{where} \quad & Q(x, \xi) \text{ is defined by } (9)\text{–}(12), \end{aligned} \tag{SAA}$$

and where $n_{\mathcal{S}} = |\mathcal{S}|$ is the number of scenarios. In our case, the SAA problem turns out to be a mixed-integer linear program, which can be solved by state-of-the-art solvers.

Let $\hat{v}(\mathcal{S})$ be the optimal value of the problem (SAA) when considering the set, $\mathcal{S}$, of scenarios. The consistency of the SAA problems have been studied by several authors (Shapiro and Homem-de Mello, 2000; Shapiro, 2021; Bastin et al., 2006). In particular, under mild conditions, $\hat{v}(\mathcal{S})$ is an asymptotically unbiased estimator of v^*, the optimal value of the true problem (5), as $\hat{v}(\mathcal{S})$ converges towards v^*, with probability one as $n_{\mathcal{S}}$ tends towards infinity. In other words, with a probability rising to one, the SAA optimal value can be made arbitrarily close to the true optimal value for a sufficiently large number of scenarios. However, for any given number, $n_{\mathcal{S}}$, of scenarios, one has $\mathbb{E}\left[\hat{v}(\mathcal{S})\right] \leq v^*$, i.e., the optimal value of the SAA problem is negatively biased, and, in practice, the required computing time grows rapidly with $n_{\mathcal{S}}$.

3.2 Appropriate Number of Scenarios

The SAA method requires to decide whether a given number of scenarios, $n_{\mathcal{S}}$, is large enough to approximate correctly the original problem, i.e., to ensure that the solution obtained is a satisfying approximation of an optimal solution of the original problem.

The optimal value of the SAA problem, $\hat{v}(\mathcal{S})$, is not necessarily a good-quality indicator with respect to the original problem, due to the SAA bias and variance of the SAA optimal value. Hence, a post-optimization validation step is needed to evaluate the quality of any SAA solution. In our study, we rely on the so-called *out-of-sample validation*, that consists in re-evaluating a first-stage SAA solution, $\hat{x}(\mathcal{S})$, with a *validation set* $\mathcal{S}_V$, containing many more scenarios than the training set $\mathcal{S}$ used to find the solution. The validation set is believed to represent the complete set of all possible scenarios, and can be used as a reference scenario set to compare the quality of different feasible solutions. The evaluation of a feasible solution x on the validation set $\mathcal{S}_V$, denoted $\hat{f}(x, \mathcal{S}_V)$, is called the *validation score*. When the gap between the SAA optimal value, $\hat{v}(\mathcal{S})$, and the validation score $\hat{f}(\hat{x}(\mathcal{S}), \mathcal{S}_V)$ is small (according to the analyst), the SAA problem can be considered as stable and the training set used large enough. As SAA solutions depend on the random scenario set $\mathcal{S}$, we build $n_{\mathcal{R}}$ replicated SAA problems with $n_{\mathcal{S}}$ scenarios each, independently generated, to illustrate better the average behavior of SAA problems with a given number of scenarios, $n_{\mathcal{S}}$. Let $\bar{v}\,(n_{\mathcal{S}}, n_{\mathcal{R}})$ be the *average optimal value* obtained over $n_{\mathcal{R}}$ such replications:

$$\bar{v}\,(n_{\mathcal{S}}, n_{\mathcal{R}}) = \frac{1}{n_{\mathcal{R}}} \sum_{r=1}^{n_{\mathcal{R}}} \hat{v}\,(\mathcal{S}_r)\,, \tag{30}$$

where $\mathcal{S}_r$, $r = 1, \ldots, n_{\mathcal{R}}$, are scenario sets of size $n_{\mathcal{S}}$, independently generated, and independent of the validation set $\mathcal{S}_V$. The corresponding *average validation score* over $n_{\mathcal{R}}$ replications, denoted $\overline{f}(n_{\mathcal{S}}, n_{\mathcal{R}}, \mathcal{S}_V)$, is

$$\overline{f}(n_{\mathcal{S}}, n_{\mathcal{R}}, \mathcal{S}_V) = \frac{1}{n_{\mathcal{R}}} \sum_{r=1}^{n_{\mathcal{R}}} \hat{f}(x^*(\mathcal{S}_r), \mathcal{S}_V), \tag{31}$$

where $x^*\,(\mathcal{S}_r)$ is the computed optimal solution of the problem (SAA), with the scenario set $\mathcal{S}_r$.

3.3 Value of the Stochastic Solution

Consider the two-stage stochastic problem (5)–(12). The incorporation of uncertainty, while making the model more realistic, comes with additional modeling questions and computational complexity, as we must decide on the random distributions to capture the uncertainty, and deal with more numerically intensive computations. It is therefore interesting to evaluate the relevance of the stochastic approach by comparing it to a simpler deterministic program. We first define the *expected value problem* (EVP) as the deterministic problem in which we replace the random vector, $\boldsymbol{\xi}$, by its expectation, $\mathbb{E}[\boldsymbol{\xi}]$:

$$\min_{x,y} f^{(1)}(x) + f^{(2)}(y, \mathbb{E}[\boldsymbol{\xi}]) \tag{32}$$

$$\text{s.t.} \quad T^{(1)}(y, t, s^{(1)}) \leq 0 \tag{33}$$

$$S^{(1)}(x, s^{(1)}) \leq 0 \tag{34}$$

$$T^{(2)}(y, s^{(2)}) \leq 0 \tag{35}$$

$$S^{(2)}(y, s^{(2)}) \leq 0 \tag{36}$$

$$x \in \mathcal{X},\ y \in \mathcal{Y}, \tag{37}$$

where

$$s^{(2)} = g(x, s^{(1)}, \mathbb{E}[\boldsymbol{\xi}]).$$

Denote by x^*_{EVP} the first-stage optimal solution found when solving (32)–(37), and assume that the two-stage stochastic program (5)–(12) has a relatively complete recourse. The *value of the stochastic solution* (VSS) (Birge and Louveaux, 2011) captures the improvement achieved when taking uncertainty into account:

$$\text{VSS} = f^{(1)}(x^*) + \mathbb{E}\left[Q(x^*, \boldsymbol{\xi}))\right] - f^{(1)}\left(x^*_{EVP}\right) - \mathbb{E}\left[Q\left(x^*_{EVP}, \boldsymbol{\xi}\right)\right]. \tag{38}$$

We again rely on the SAA approach to approximate the true VSS (38), defining the *SAA VSS* with respect to the set of scenarios $\mathcal{S}$ and the validation set $\mathcal{S}_V$ as

$$\widehat{\text{VSS}}(\mathcal{S}, \mathcal{S}_V) = \hat{f}\left(x^*(\mathcal{S}), \mathcal{S}_V\right) - \hat{f}\left(x^*_{EVP}, \mathcal{S}_V\right). \tag{39}$$

In other terms, the true solution x^* is replaced by the SAA solution $x^*(\mathcal{S})$, and the approximate VSS is computed as the difference of the validation scores computed at $x^*(\mathcal{S})$ and x^*_{EVP}. We can also compute the relative approximate VSS as

$$\widehat{\text{VSS}}_{\%}(\mathcal{S}, \mathcal{S}_V) = \widehat{VSS}(\mathcal{S}, \mathcal{S}_V) / \hat{f}\left(x^*_{EVP}, \mathcal{S}_V\right). \tag{40}$$

4 Numerical Study

We now illustrate our approach on various numerical experiments. Subsection 4.1 presents the realistic instances of the two-stage stochastic optimization problem we are addressing, together with the considered test data to conduct our numerical study. The aim of the numerical study is threefold. First, in Subsection 4.2, we seek the appropriate number of scenarios in order to apply the SAA method. Second, in Subsection 4.3, we compute the value of the stochastic solution for different uncertainty amplitudes in order to assess the benefit from taking account of the uncertainty via two-stage stochastic programming. Third, we study in Subsection 4.4 the effect of chance constraints on the value of the stochastic solution, and on the solution quality. All numerical tests are conducted on a Windows platform with an Intel i5-10310U and 16 GB RAM using the solver CPLEX 22.1.0.0.

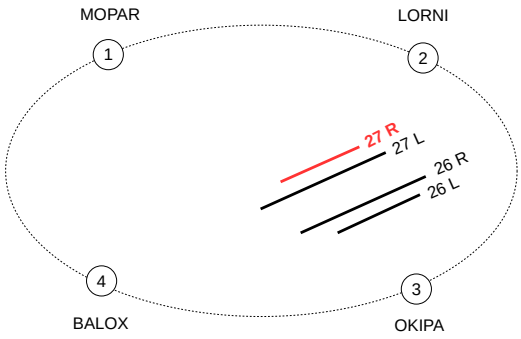

Fig. 2 Simplified scheme of the four IAFs surrounding the four runways of CDG airport

4.1 Instances and Test data

We focus on Paris Charles-de-Gaulle airport (CDG) and its northern landing runway (named 27R), depicted in Figure 4, along with its surrounding IAFs. We use the five instances, of $n = 10$ aircraft each, described in Khassiba et al. (2022). They correspond to aircraft planning to land on the northern runway 27R, and to cross the two IAFs, MOPAR or LORNI, between 5:59 AM and 6:59 AM, on May 5, 2015. Instance characteristics are summarized in Table 2. We assume that time deviations of the IAF actual times, for all aircraft, are independent and normally distributed, with zero mean of variance σ^2. Additional test data are summarized in Table 3. Delay and advance unit costs, in euros per second, are the same as in Khassiba et al. (2022, Appendix C).

Table 2 Instance characteristics

Instance id	559_618	607_623	619_634	624_640	634_659
$\lvert\mathcal{A}\rvert$	10	10	10	10	10
Time span	10 min 30 s	8 min 42 s	8 min 30 s	8 min 4 s	12 min 29 s
$\lvert\mathcal{A}_A\rvert$	6	4	3	5	7
$\lvert\mathcal{A}_G\rvert$	4	6	7	5	3
# Medium (M)	4	6	7	7	7
# Heavy (H)	6	4	3	3	3
# assigned to IAF 1	6	5	5	4	3
# ass. to IAF 2	4	5	5	6	7

Table 3 Test data

Parameter	Definition	Test values
$\overline{d}^G$	Maximal delay at-gate, seconds	900
$\underline{d}_a^R$	Maximal advance en-route, seconds	60
$\overline{d}_a^R$	Maximal delay en-route, seconds	300
$\underline{d}_a^T$	Maximal advance approach, seconds	0
$\overline{d}_a^T$	Maximal delay approach, seconds	1200
r	Rerouting time to change IAF, seconds	300
$\underline{S}$	Minimal IAF time separation, seconds	72
$\hat{V}_a^1$	Unconstrained flight time from MOPAR to runway, seconds	780
$\hat{V}_a^2$	Unconstrained flight time from LORNI to runway, seconds	660
σ	Standard deviation of the normal random deviation ξ, seconds	60, 120
$n_{\mathcal{S}}$	Number of scenarios in the SAA problem	10, 50, 100, 200
$n_{\mathcal{S}_V}$	Number of scenarios in the validation set	1000
$n_{\mathcal{R}}$	Number of replications	20

4.2 Appropriate Number of Scenarios

We consider the problem (SAA), and explore an increasing number of scenarios $n_{\mathcal{S}} = 10, 50, 100, 200$, to determine the number of scenarios required to accurately enough approximate the true problem. For each value of $n_{\mathcal{S}}$, we solve $n_{\mathcal{R}} = 20$ independently generated replications of the SAA problem. In our experiments, the scenario sets are built incrementally, i.e., for a given replication $r = 1, 2, \ldots, n_{\mathcal{R}}$ and two scenario sets $\mathcal{S}'_r$ and $\mathcal{S}_r$, such that $n_{\mathcal{S}'_r} < n_{\mathcal{S}_r}$, we have $\mathcal{S}'_r \subset \mathcal{S}_r$. The optimal solution of each replication is then evaluated on the same validation set $\mathcal{S}_V$, with $n_{\mathcal{S}_V} = 1,000$. Figure 3 focuses on instance 559_618 and plots the average optimal value (30) and the average validation score (31) for an increasing number of scenarios, using boxplots to exhibit the variability of the optimal value $\hat{v}(\mathcal{S})$ and the validation score $\hat{f}(\hat{x}(\mathcal{S}), \mathcal{S}_V)$ over the replications.

As $n_{\mathcal{S}}$ grows, we observe that the average optimal value increases, whereas the average validation score decreases, while their variances decrease. This behavior can be expected as a SAA problem with a scenario set $\mathcal{S}' \subset \mathcal{S}$ can be viewed as a relaxation of the SAA problem with a scenario set $\mathcal{S}$ with respect to the first-stage decision x. However, due to the variability of the second-stage cost, the SAA optimal value is not constrained to be monotonically increasing with respect to the number of scenarios, as reflected by the whiskers of the boxplots, while this variability decreases as $n_{\mathcal{S}}$ increases. The evolution of the validation score, both in terms of average and variance, illustrates the convergence of the SAA optimal value towards the true optimal value when $n_{\mathcal{S}}$ rises, in line with consistency analysis results (Shapiro, 2021). More specifically, we observe that, as the number of scenarios increases, the variances of the optimal value and validation score decrease, as well as the bias between the SAA and true optimal values, produced by the optimization over a finite sample size. For 200 scenarios, the variance of the validation score can be

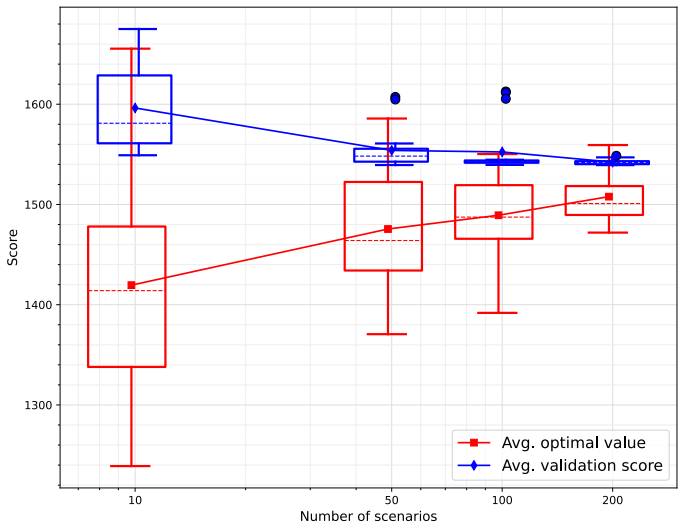

Fig. 3 Objective function's optimal value and validation score as functions of the number of scenarios, for the instance 559_618

neglected, and the its average is close to the average SAA optimal value. Due to the numerical costs experienced with 200 scenarios (around 9 minutes on average to find the optimal solution of one replication), we decided not to increase the number of scenarios furthermore, and use $n_{\mathcal{S}} = 100$ as the number of scenarios for our subsequent tests.

4.3 Value of the Stochastic Solutions

Fixing the number of scenarios to $n_{\mathcal{S}} = 100$, we solve $n_{\mathcal{R}} = 20$ replications of the problem (SAA), for each of the five studied instances, and report the main results in Table 4. For each instance, we test two values of the standard error σ of the normally distributed random deviations, 60 and 120 seconds, corresponding to low and high uncertainty levels. We report in the column "CPU time" the computing time, in seconds, to find an optimal solution, averaged over the $n_{\mathcal{R}}$ replications, and the average validation score (31) in column "Validation score". The SAA VSS (39) and its relative counterpart (40), averaged over the $n_{\mathcal{R}}$ replications, are reported in columns "$\widehat{\text{VSS}}$" and "$\widehat{\text{VSS}}$ (%)", respectively. The ratio of aircraft that changed their IAF, averaged over all replications, is reported in column "Avg IAF changes". The number of different sequences at IAF 1, IAF 2, and runway, in the optimal solutions

of the $n_{\mathcal{R}}$ replications, are listed in columns "# different sequences IAF 1", "IAF 2", and "RWY", respectively.

Table 4 Results summary of the stochastic solutions of all instances

Instance	σ (s)	CPU time (s)	Val. score (euros)	$\widehat{\text{VSS}}$ (euros)	$\widehat{\text{VSS}}$ (%)	Avg IAF changes	# different sequences IAF 1	IAF 2	RWY
10_559_618	60	138.77	1,552.38	-216.79	-12.25%	19%	2	2	2
	120	212.09	2,782.65	-478.32	-14.67%	30%	1	1	1
10_607_623	60	78.78	1,070.92	-295.27	-21.61%	1%	2	2	2
	120	106.62	1,997.39	-448.40	-18.33%	10%	4	4	5
10_619_634	60	178.53	1,062.28	-22.04	-2.03%	0%	2	2	3
	120	698.71	1,899.01	-59.70	-3.05%	0%	2	2	6
10_624_640	60	575.54	944.40	-136.14	-12.60%	1%	2	2	2
	120	660.24	1,673.17	-206.55	-10.99%	16%	4	3	7
10_634_659	60	37.63	670.34	-108.51	-13.93%	5%	1	2	2
	120	177.61	1,445.17	-266.61	-15.58%	10%	1	2	2

The increase in computational time alongside the uncertainty level exhibits that the problem then becomes more expensive to solve, even though the number of scenarios is fixed. Moreover, greater uncertainty leads to higher deviation costs, captured by the validation scores. Negative values of the stochastic solution, ranging from -2.03% to -21.61%, illustrate the benefit from taking into account uncertainty through two-stage stochastic programming. Moreover, the increase of the VSS in absolute value with the level of uncertainty suggests that the benefit of two-stage stochastic programming is greater for high uncertainty. Modifying the IAF assignment, by rerouting flights during the en-route phase, appears to be an efficient measure to hedge against uncertainty, as the average number of IAF changes increases as uncertainty grows, while deterministic expected value solutions do not propose any IAF change. Note that for σ equal to 60 seconds, most of the instances present two different sequences at each IAF and on the runway, across the $n_{\mathcal{R}}$ replications. This comforts the selection of $n_{\mathcal{S}} = 100$ as an appropriate number of scenarios. On the other hand, the higher uncertainty level, generated by fixing σ to 120 seconds, leads to a larger number of different sequences, in most cases, and more scenarios could be required to stabilize the solution.

4.4 Effect of the Chance Constraints

To study the effect of chance constraints, we run additional experiments with the same setup as in the previous Subsection 4.3, and the addition of the chance constrains (29), with $\alpha = 0.9$. Table 5 provides the values of the minimal IAF time separation, in the original case (without chance constraints) and when chance constraints are

included, with $\alpha = 0.9$, and the uncertainty level, σ, equal to 60 or 120 seconds. A summary of the results is provided in Table 6.

Table 5 Minimal IAF time separations (s) for the studied values of α and σ

$\underline{S}$	$\underline{S} + F^{-1}_{\psi_{ab}}(\alpha)$	
	$\alpha = 0.9$, $\sigma = 60$ s	$\alpha = 0.9$, $\sigma = 120$ s
72.0	180.7	289.5

Table 6 Results summary of the stochastic solutions of all instances with chance constraints ($\alpha = 0.9$)

Instance	σ (s)	CPU time (s)	Val. score (euros)	$\widehat{\text{VSS}}$ (euros)	$\widehat{\text{VSS}}$ (%)	Avg IAF changes	# different sequences IAF 1	IAF 2	RWY
10_559_618	60	225.94	2,361.37	-94.96	-3.87%	26%	2	2	2
	120	113.83	4,855.63	-35.94	-0.73%	30%	2	2	4
10_607_623	60	324.40	1,769.40	-246.86	-12.24%	12%	3	4	5
	120	398.99	3,108.35	-118.49	-3.67%	20%	3	2	4
10_619_634	60	652.26	1,146.99	-76.51	-6.25%	0%	1	1	3
	120	1256.40	2,480.56	-36.36	-1.44%	20%	4	2	4
10_624_640	60	649.15	982.73	-37.51	-3.68%	11%	2	3	4
	120	646.20	1,982.12	-39.69	-1.96%	12%	2	2	2
10_634_659	60	164.51	929.57	-47.60	-4.87%	10%	3	1	3
	120	433.82	2,427.54	-15.61	-0.64%	23%	3	2	4

A comparison with Table 4 reveals that the inclusion of change constraints usually leads to higher computing times, suggesting that the problem with a buffered IAF separation is more difficult to solve. A possible explanation is that buffered IAF separations of 3 up to more than 4.5 minutes, as computed in Table 5, make difficult to find feasible sequences since in our experimental settings, described in Table 4.1, the maximal possible advance and delay at the IAF for a given aircraft are 1 minute and 5 minutes, respectively. This also contributes to produce more IAF changes, that offer additional en-route delays (recall that one IAF change represents 5 minutes of en-route delay), and larger validation scores, i.e., larger time deviation costs. This is consistent with the fact that buffered separation corresponds to a conservative approach, hedging against uncertainty. However, for the case of instance 10_559_618 with σ equal to 120 seconds, the average computing time is the smallest over all cases involving this instance, with and without chance constraints, which might be explained by a set of feasible solutions being very small due to the large IAF separation requirement. The associated validation score is also the highest over all instances, highlighting that the solutions produced are averse to the risk of facing too small separations.

The chance-constrained variant of the problem presents smaller VSS in absolute value than the original formulation in the problem (SAA). This suggests that, when buffered IAF separations are used, there is a smaller room for the two-stage programming to improve on the deterministic EVP solutions, compared to the case with a basic IAF separation. This conclusion is consistent with the results obtained by Khassiba et al. (2020).

In summary, using buffered IAF separation seems inefficient to hedge against uncertainty for the problem of stochastic extended aircraft arrival scheduling with total deviation cost minimization, as validation scores are higher for both the stochastic and the deterministic EVP solutions.

5 Conclusions and Perspectives

This chapter introduced a high-level multi-stage stochastic optimization formulation to manage aircraft arrivals in the context of extended arrival manager systems, for which uncertainty is significant when predicting expected times to start the approach phase and landing times. It first considered a general setup involving several air network points of interest, and then presented a review of recent developments for the two-stage special case, which corresponds to recent studies on the aircraft arrival management problem taking account of practical operational constraints. Numerical experiments conducted on realistic instances based on Paris-Charles de Gaulle arrival data exhibited that the stochastic solutions are more robust than their deterministic counterparts, and can be obtained within a reasonable computing time budget using a limited number of randomly generated scenarios. Introducing chance constraints at the first stage to hedge against uncertainty led to an increase in required computing time and tended to yield overly conservative solutions. As a result, for this particular problem, this approach should not be prioritized.

Several avenues for future research were evoked, including the possibility to solve more realistic problems, relying for instance on a multi-stage formulation, and a better representation of the uncertainty affecting on-ground aircraft. More work on scenario generation and selection could be pursued to improve the solution quality while using a limited number of scenarios, allowing computing time reduction. Quantifying uncertainty in terms of random variables remains a challenging task due to the intricate interplay of random time deviations and air control orders in real delay data. To address this, adopting a distributionally robust optimization framework could provide a more accurate representation of the available information and lead to better results. Furthermore, extending the solution to a rolling horizon framework would be beneficial (Abba Rapaya et al., 2021; Furini et al., 2015) This advancement would facilitate the consideration of larger aircraft sequences and better reflect the dynamic nature of air traffic.

6 Acknowledgments

We would like to express our deepest gratitude to Bernard Gendron, who played a major role in the development of this research. He will be deeply missed. We also would like to thank two anonymous referees for their valuable comments. The work of Fabian Bastin is supported by the Natural Sciences and Engineering Research Council of Canada [Discovery Grant 2022-04400].

References

Abba Rapaya S, Notry P, Delahaye D (2021) Coordinated sequencing of traffic on multiple en-route constraint points. In: Electronic Navigation Research Institute (ed) Air Traffic Management and Systems IV, Springer, Singapore, pp 41–57

Antolovic D, Franjkovic D (2020) Calculation of airplane wake turbulence re-categorisation effects. Transportation Research Procedia 51:179–189, DOI 10.1016/j.trpro.2020.11.020

Balakrishnan H, Chandran BG (2010) Algorithms for scheduling runway operations under constrained position shifting. Operations Research 58(6):1650–1665, DOI 10.1287/opre.1100.0869

Bastin F, Cirillo C, Toint PhL (2006) Convergence theory for nonconvex stochastic programming with an application to mixed logit. Mathematical Programming 108(2–3):207–234, DOI 10.1007/s10107-006-0708-6

Beasley JE, Krishnamoorthy M, Sharaiha YM, Abramson D (2000) Scheduling aircraft landings: The static case. Transportation Science 34(2):180–197, DOI 10.1287/trsc.34.2.180.12302

Bennell JA, Mesgarpour M, Potts CN (2011) Airport runway scheduling. 4OR 9(2):115–138, DOI 10.1007/s10288-011-0172-x

Birge JR, Louveaux F (2011) Introduction to stochastic programming. Springer, 2nd edition

Bolić T, Ravenhill P (2021) SESAR: The past, present, and future of European air traffic management research. Engineering 7(4):448–451, DOI https://doi.org/10.1016/j.eng.2020.08.023

Bradley S, Hax A, Magnanti TL (1977) Applied Mathematical Programming. Addison-Wesley, available on line: http://web.mit.edu/15.053/www/AMP.htm

Breitsamter C (2011) Wake vortex characteristics of transport aircraft. Progress in Aerospace Sciences 47:89–134, DOI 10.1016/j.paerosci.2010.09.002

Cook AJ, Tanner G (2015) European airline delay cost reference values. Tech. rep., EUROCONTROL Performance Review Unit, University of Westminster, London, United Kingdom

Dear RG (1976) The dynamic scheduling of aircraft in the near terminal area. Tech. Rep. FTL Report R76-9, Massachusetts Institute of Technology, Cambridge, MA, USA

Dear RG, Sherif YS (1991) An algorithm for computer assisted sequencing and scheduling of terminal area operations. Transportation Research Part A 25(2):129–139, DOI 10.1016/0191-2607(91)90132-A

Furini F, Kidd MP, Persiani CA, Toth P (2015) Improved rolling horizon approaches to the aircraft sequencing problem. Journal of Scheduling 18(5):435–447, DOI 10.1007/s10951-014-0415-8

Gerz T, Holzäpfel F, Darracq D (2002) Commercial aircraft wake vortices. Progress in Aerospace Sciences 38(3):181–208, DOI 10.1016/S0376-0421(02)00004-0

Hasevoets N, Conroy P (2010) Arrival Manager - Implementation guidelines and lessons learned. Tech. rep., EUROCONTROL, Brussels, Belgium, URL `https://www.skybrary.aero/bookshelf/books/2416.pdf`

Huo Y, Delahaye D, Sbihi M (2021) A probabilistic model based optimization for aircraft scheduling in terminal area under uncertainty. Transportation Research Part C 132:103374, DOI 10.1016/j.trc.2021.103374

Ikli S, Mancel C, Mongeau M, Olive X, Rachelson E (2021) The aircraft runway scheduling problem: A survey. Computers & Operations Research 132:105336, DOI doi.org/10.1016/j.cor.2021.105336

Itoh E, Brown M, Senoguchi A, Wickramasinghe NK, Fukushima S (2017) Future arrival management collaborating with trajectory-based operations. In: Electronic Navigation Research Institute (ed) Air Traffic Management and Systems II: Selected Papers of the 4th ENRI International Workshop, 2015, Springer, Tokyo, Japan, pp 137–156, DOI 10.1007/978-4-431-56423-2_7

Itoh E, Miyazawa Y, Finke M, Rataj J (2021) Macroscopic analysis to identify stage boundaries in multi-stage arrival management. In: Electronic Navigation Research Institute (ed) Air Traffic Management and Systems IV, Springer, Singapore, Singapore, pp 59–76

Khassiba A, Bastin F, Gendron B, Cafieri S, Mongeau M (2019) Extended aircraft arrival management under uncertainty: A computational study. Journal of Air Transportation 27(3):131–143, DOI 10.2514/1.D0135

Khassiba A, Bastin F, Cafieri S, Gendron B, Mongeau M (2020) Two-stage stochastic mixed-integer programming with chance constraints for extended aircraft arrival management. Transportation Science 54(4):897–919, DOI 10.1287/trsc.2020.0991

Khassiba A, Cafieri S, Bastin F, Gendron B, Mongeau M (2022) Two-stage stochastic programming models for the extended aircraft arrival management problem with multiple pre-scheduling points. Transportation Research Part C 142:103769, DOI 10.1016/j.trc.2022.103769

Kistan T, Gardi A, Sabatini R, Ramasamy S, Batuwangala E (2017) An evolutionary outlook of air traffic flow management techniques. Progress in Aerospace Sciences 88:15–42, DOI 10.1016/j.paerosci.2016.10.001

Liu M, Liang B, Zheng F, Chu C, Chu F (2018) A two-stage stochastic programming approach for aircraft landing problem. In: 15th International Conference on Service Systems and Service Management (ICSSSM), pp 1–6, DOI 10.1109/ICSSSM.2018.8465107

Psaraftis HN (1978) A dynamic programming approach to the aircraft sequencing problem. Tech. Rep. R78-4, Massachusetts Institute of Technology, Cambridge, MA, USA

Samà M, D'Ariano A, D'Ariano P, Pacciarelli D (2014) Optimal aircraft scheduling and routing at a terminal control area during disturbances. Transportation Research Part C 47:61–85, DOI 10.1016/j.trc.2014.08.005

Scala P, Mota MM, Wu CL, Delahaye D (2021) An optimization–simulation closed-loop feedback framework for modeling the airport capacity management problem under uncertainty. Transportation Research Part C 124:102937, DOI 10.1016/j.trc.2020.102937

Shapiro A (2021) Statistical inference. In: Shapiro A, Dentcheva D, Ruszczyński A (eds) Lectures on Stochastic Programming: Modeling and Theory, Third Edition, Springer, Philadelphia, PA, USA, chap 5, pp 151–221

Shapiro A, Homem-de Mello T (2000) On the rate of convergence of optimal solutions of Monte Carlo approximations of stochastic programs. SIAM Journal on Optimization 11(1):70–86, DOI 10.1137/S1052623498349541

Shone R, Glazebrook K, Zografos KG (2021) Applications of stochastic modeling in air traffic management: Methods, challenges and opportunities for solving air traffic problems under uncertainty. European Journal of Operational Research 292(1):1–26, DOI 10.1016/j.ejor.2020.10.039

Sölveling G, Clarke JP (2014) Scheduling of airport runway operations using stochastic branch and bound methods. Transportation Research Part C 45:119–137, DOI 10.1016/j.trc.2014.02.021

Sölveling G, Solak S, Clarke JP, Johnson E (2011) Runway operations optimization in the presence of uncertainties. Journal of Guidance, Control, and Dynamics 34(5):1373–1382, DOI 10.2514/6.2010-9252

Tielrooij M, Borst C, Van Paassen MM, Mulder M (2015) Predicting arrival time uncertainty from actual flight information. In: Proceedings of the 11th USA/Europe Air Traffic Management Research and Development Seminar, FAA/EUROCONTROL, pp 577–586

Vié MS, Zufferey N, Leus R (2022) Aircraft landing planning under uncertain conditions. Journal of Scheduling 25(2):203–228, DOI 10.1007/s10951-022-00730-0

Appendix: Summary of notations used

Sets	
	Multi-stage formulation
$\mathcal{A}^{(k)}$	index set of aircraft at stage k
$\mathcal{A}_A^{(k)}$	index set of airborne aircraft at stage k
$\mathcal{A}_G^{(k)}$	index set of on-ground aircraft at stage k
$\mathcal{I}^{(k)}$	index set of possible aircraft routes at stage k
$\mathcal{X}^{(k)}$	feasible set for the decision vector $x^{(k)}$
	Two-stage formulation
$\mathcal{A}$	index set of aircraft
$\mathcal{A}_G$	index set of on-ground aircraft
$\mathcal{A}_A$	index set of airborne aircraft
$\mathcal{I}$	index set of IAFs
$\mathcal{A}^{i^*}$	index set of aircraft whose initial IAF is $i^* \in \mathcal{I}$
$\mathcal{A}_G^{i^*}$	index set of on-ground aircraft whose initial IAF is $i^* \in \mathcal{I}$
$\mathcal{A}_A^{i^*}$	index set of airborne aircraft whose initial IAF is $i^* \in \mathcal{I}$
$\mathcal{X}$	feasible set for the first-stage decision vector
$\mathcal{Y}$	feasible set for the second-stage decision vector
$\mathcal{S}$	set of uncertainty scenarios used for optimization
$\mathcal{S}_r$	rth-replication set of uncertainty scenarios used for optimization
$\mathcal{S}_V$	set of uncertainty scenarios used for validation

Parameters	
	Multi-stage formulation
K	number of stages
$n^{(k)}$	number of aircraft at stage k
$s^{(k)}$	state vector at stage k
$s_a^{(k)}$	ath component of the state vector at stage k
$p_a^{(k)}$	position of aircraft a at stage k
$r_a^{(k)}$	current (at stage k) reference route of aircraft a
$v_a^{(k)}$	speed of aircraft a at stage k
$\kappa_a^{(k)}$	status (on-ground or airborne) of a at stage k
$\chi_a^{(k)}$	other characteristics of aircraft a such as its wake-vortex turbulence category
$\boldsymbol{\xi}^{(k)}$	random vector capturing the uncertainty affecting the problem at stage k
	Two-stage formulation
P_a^i	planned IAF time of aircraft a at an IAF i
P_a^{TOT}	planned take-off time of aircraft $a \in \mathcal{A}_G$

E_a^i	earliest time for aircraft a to reach IAF i
L_a^i	latest time for aircraft a to reach IAF i
r^{ij}	delay due to rerouting from IAF i to IAF j
$\hat{V}_a^O$	unimpeded flight time from the origin airport of aircraft $a \in \mathcal{A}_G$
$\hat{V}_a^i$	unimpeded time for aircraft a to fly from IAF i to the landing runway
$\underline{V}_a^i$	minimal time for aircraft a to fly from IAF i to the landing runway
$\overline{V}_a^i$	maximal time for aircraft a to fly from IAF i to the landing runway
$\overline{d}^G$	maximum delay on-ground
$\underline{d}_a^R$	maximal possible time saving for aircraft a during en-route phase
$\overline{d}_a^R$	maximal possible delay for aircraft a during en-route phase
$\underline{d}_a^T$	maximal possible time saving for aircraft a during approach phase
$\overline{d}_a^T$	maximal possible delay for aircraft a during approach phase
$\underline{S}$	minimal time separation between two consecutive aircraft at IAF
$\underline{S}_{ab}$	minimal final-approach time separation between leading aircraft a and following aircraft b
$\boldsymbol{\xi}_a$	random variable of IAF time deviation of aircraft a
ξ_a	realization of the random variable, IAF time deviation of aircraft a
M_{ab}	big-M constant enabling/disabling the separation constraint at IAFs between aircraft a and b
M_{ab}^L	big-M constant enabling/disabling the separation constraint at the runway between aircraft a and b
σ	standard deviation of the normal random deviation $\boldsymbol{\xi}$
α	desired probability of separation between any pair of aircraft over their IAF
$\boldsymbol{\psi}_{ab}$	random variable defined as $\boldsymbol{\psi}_{ab} = \boldsymbol{\xi}_a - \boldsymbol{\xi}_b$
$n_{\mathcal{S}}$	number of scenarios in uncertainty scenario set $\mathcal{S}$
$n_{\mathcal{S}_V}$	number of scenarios in validation scenario set $\mathcal{S}_V$
$n_{\mathcal{R}}$	number of replications of uncertainty scenario sets used for optimization

Functions	
	Multi-stage formulation
$f^{(k)}$	cost function at stage k
$S^{(k)}$	separation-constraint mapping at stage-(k+1) target points
$T^{(k)}$	time-window constraint mapping at stage-(k+1) target points
$g^{(k)}$	state transition function from stage k to stage $k+1$
$V^{(k)}$	optimal value function at stage k
	Two-stage formulation
Q	recourse cost
f_a^{G}	cost function of the time deviation at gate of aircraft $a \in \mathcal{A}_G$
f_a^{R}	cost function of the time deviation en route of aircraft a
f_a^{T}	cost function of the time deviation in approach of aircraft a

$F_{\psi_{ab}}$	probability distribution function of random variable ψ_{ab}
$\hat{f}$	objective function of the SAA problem
$\bar{f}$	average validation score over a number of replications
$\hat{v}$	optimal value of the SAA problem
v^*	optimal value of the true problem
$\bar{v}$	average optimal value over a number of replications of the SAA problem

Decision vectors/variables	
	Multi-stage formulation
$x^{(k)}$	decision vector at stage k
$z^{(k)}$	vector of target-time variables (associated to stage-(k+1) target point)
$t^{(k)}$	vector of target take-off time variables for on-ground aircraft at stage k
$\delta^{(k)}$	vector of sequencing variables of aircraft at stage-(k+1) target point
$\zeta^{(k)}$	vector of the aircraft route assignment variables at stage k
	Two-stage formulation
x	decision vector in the first-stage problem
$\hat{x}(\mathcal{S})$	feasible (first-stage) decision vector of the SAA problem with scenario set $\mathcal{S}$
$x^*(\mathcal{S})$	optimal (first-stage) decision vector of the SAA problem with scenario set $\mathcal{S}$
x^*_{EVP}	optimal (first-stage) decision vector of the expected value problem
z_a	target IAF time of aircraft $a \in \mathcal{A}$
t_a	target take-off time of aircraft $a \in \mathcal{A}_G G$
δ_{ab}	sequencing variable of aircraft pair $(a, b) \in \mathcal{A} \times \mathcal{A}$
ζ^i_a	assignment variable of aircraft a to IAF i
ϕ_{ab}	same-IAF indicator variable for aircraft pair $(a, b) \in \mathcal{A} \times \mathcal{A}$
y	decision vector in the second-stage problem
y_a	target landing time of aircraft $a \in \mathcal{A}$